Visible Region Magnetic Linear Dichroism Spectra of Ferrocytochrome *c* and Deoxymyoglobin: Demonstration of a New Tool for the Study of Metalloproteins

Jim Peterson,*,† Linda L. Pearce,‡ and Emile L. Bominaar†

Contribution from the Department of Chemistry, Carnegie Mellon University, 4400 Fifth Avenue, Pittsburgh, Pennsylvania 15213, and Department of Pharmacology, University of Pittsburgh School of Medicine, Pittsburgh, Pennsylvania 15261

Received January 19, 1999

Abstract: Using a newly reconfigured magnetooptical instrument, originally constructed for magnetic circular dichroism experiments, it has been shown that the ferrous hemoprotein derivatives ferrocytochrome *c* ($S = 0$) and deoxymyoglobin ($S = 2$) exhibit readily detectable magnetic-field-induced linear dichroism (MLD) signals in the near-ultraviolet-to-visible region. To our knowledge, this is the first time MLD spectra have been reported for metalloprotein samples. The results suggest that MLD exhibits selectivity toward the transition type and chromophore spin which is complementary to that of the corresponding magnetic circular dichroism. Not surprisingly, the band patterns detected in the two magnetooptical spectroscopies are qualitatively different. The second-derivative dispersion associated with the ferrocytochrome *c* Q-band MLD and the linear variation in signal intensity with the square of the field observed for both non-Kramers hemoprotein derivatives studied under nonsaturating conditions are fully in accord with theoretical predictions. These observations establish unambiguously that an MLD effect has indeed been measured. The magnitudes of the ferrocytochrome *c* excited-state orbital momenta inferred from a combination of MLD and MCD measurements are substantially lower than those previously estimated by consideration of MCD and absorption data, but are in keeping with the available results of the most detailed theoretical calculations concerning metalloporphyrins. Since many other paramagnetic metalloprotein derivatives and model compounds are anticipated to yield MLD spectra, a broad range of potential applications is envisaged.

Introduction

It has previously been shown in the case of matrix-isolated atomic examples[1,2] that the magnetooptical spectroscopic methods known as magnetic circular dichroism (MCD) and magnetic linear dichroism (MLD) provide essentially complementary information relevant to the assignment of electronic transitions. The complementarity stems from the differing selection rules associated with the two techniques (as illustrated in Figure 1), resulting in the detectability of $\Delta M_L = 0$ transitions by MLD, but not by MCD. While it is clear in the case of the particularly simple example of an atomic $^1S \rightarrow {}^1P$ transition shown that the energies of the magnetic sublevels can be determined by a combination of absorption and MCD spectroscopies, in general, this will not be so. Additional factors must be taken into consideration, such as the presence of zero-field splitting and the possibility of magnetic-field-induced mixing of molecular states. It follows that the concerted application of MCD and MLD spectroscopies to the study of metalloprotein derivatives and model compounds can reasonably be anticipated to afford significant additional insight into their electronic structures as already demonstrated for atoms. In contrast to the quite extensive literature concerning the MCD spectra of metalloproteins, especially in the ultraviolet-to-near-infrared region of the spectrum,[3−11] there appear to be no previous reports of the MLD spectra of such systems.

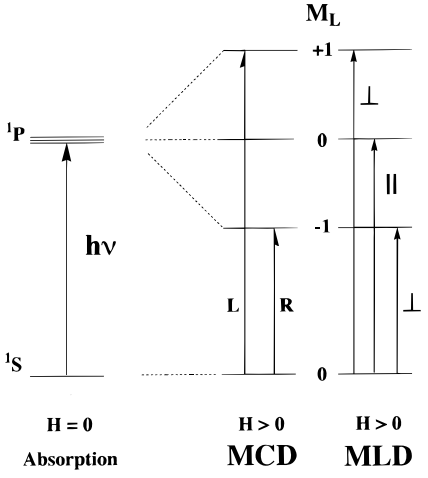

Figure 1. Illustration of the selection rules for MCD and MLD electric-dipole-allowed transitions using an atomic example. Following the application of the magnetic field (H), the excited-state levels undergo a Zeeman splitting ($\Delta E = \mu_B H M_L$). For MCD, $\Delta M_L = +1$ and -1 correspond to the absorption of left and right circularly polarized light, respectively. For MLD, $\Delta M_L = 0$ and ± 1 correspond to the absorption of parallel and perpendicular plane (i.e., linearly) polarized light, respectively.

* To whom correspondence should be addressed. Phone: (412) 268-5670. Fax: (412) 268-1061. E-mail: jamesp@andrew.cmu.edu.

† Carnegie Mellon University.

‡ University of Pittsburgh School of Medicine.

(1) Vala, M.; Rivoal, J.-C.; Grisolia, C.; Pyka, J. *J. Chem. Phys.* **1985**, *82*, 4376−4377.

(2) Rivoal, J. C.; Zoueu, J.; Blanchard, X.; Nahoum, R.; Eyring, M.; Pyka, M.; Vala, M. *J. Chem. Phys.* **1994**, *101*, 2684−2692.

10.1021/ja990174k CCC: $18.00
Published on Web 06/15/1999

A combined cryomagnet−spectrometer system suitable for recording MLD spectra of samples prepared as frozen glasses has been assembled from commercially available customized components with minor modifications. This instrument has been used to investigate the Q-band MLD spectra of ferrocytochrome *c* ($S = 0$) and deoxymyoglobin ($S = 2$), these particular hemoprotein derivatives being selected as benchmark examples of strong chromophores exhibiting a well-characterized transition. The ferrocytochrome *c* spectra have been analyzed within the framework of a recently developed theory for the MLD of molecular systems.[12,13] This analysis serves to firmly establish that the MLD effect can readily be measured for some metalloprotein samples and illustrates the feasibility of extracting information from such data.

Unlike the case for ferrocytochrome *c*, the deoxymyoglobin MLD spectra are strongly temperature dependent, as expected for a chromophore with a paramagnetic ground state. Intriguingly, the present MLD spectra differ qualitatively from the MCD spectra in that they appear not to reveal the presence of some transitions which are predominantly d−d in nature. Thus, straightforward visual comparison of the two kinds of magneto-optical spectra may prove to be an advantageous diagnostic procedure in the assignment of electronic transitions. The deoxymyoglobin MLD signals are significantly more intense than those exhibited by the low-spin ferric hemes we have investigated thus far. This observation suggests that MLD spectroscopy may be of considerable utility in the study of active-site $S > {}^1/_2$ centers in multicomponent metalloproteins where additional electron-transfer sites, especially cytochromes, are present. Finally, the current study indicates that the magneto*kinetic* effect previously reported for the CO rebinding rate of hemoglobin[14] is entirely, or at least in part, a *static* magnetic linear dichroism, like that we now report.

Methodology

Sample Preparation. Ferricytochrome *c* (equine heart, type VI) and metmyoglobin (equine skeletal muscle) were purchased from Sigma. Using all reagents as supplied by their manufacturers, ferrous derivatives were prepared in the following manner. The required hemoprotein was dissolved in 0.1 M *N*-(2-hydroxyethyl)piperazine-*N*′-(2-ethanesulfonate) (Fisher) buffer at pH 7.4. Next, glycerol (Fisher) was added to 50% (v/v) to ensure formation of a glass upon subsequent freezing. An aliquot (40−60 μL) of the semiaqueous solution was then transferred to a quartz cuvette (0.3−0.5 mm path length) and reduced with excess sodium dithionite (EM Science). Within 1 min of reduction, the sample was frozen by insertion into the instrument's cryomagnet, where it was immersed in liquid helium. Ferrocytochrome *c* and deoxymyoglobin concentrations were determined by room-temperature electronic absorption employing the extinction coefficients $\epsilon_{550} = 27.7\ \mathrm{mM^{-1}\ cm^{-1}}$ [15] and $\epsilon_{560} = 13.8\ \mathrm{mM^{-1}\ cm^{-1}}$,[16] respectively.

Experimental Configuration and Instrumentation. In the MLD experiment, a beam of plane (linearly) polarized light, with its electric vector alternately aligned parallel and perpendicular to the applied field, is passed through the sample. The measured signal is the difference between the absorption of parallel and perpendicular polarized light: $\Delta A_{\mathrm{MLD}} = A_{\parallel} - A_{\perp}$. Spectra are reported in terms of differential extinction coefficients (i.e., differential absorptivities, where $\Delta\epsilon_{\mathrm{MLD}} = \Delta A_{\mathrm{MLD}}$/concentration/path length).

Spectra were recorded using an Aviv Associates (Lakewood, NJ) 41DS circular dichroism (CD) spectrometer in conjunction with a Cryomagnetics Inc. (Oak Ridge, TN) combined superconducting magnet and optical cryostat. The CD spectrometer was modified to operate in linear dichroism (LD) mode by insertion of an achromatic quarter-wave retardation plate between the photoelastic modulator and sample—the configuration first suggested by Nordén and Davidsson.[17] The cryomagnet, constructed with two perpendicular optical paths, could be rotated to allow the applied magnetic field to be aligned either parallel or perpendicular to the optical axis of the spectrometer. The sample was mounted on the end of a probe which could be rotated to allow transmission of the polarized light beam through the optical path of the cuvette with either orientation of the applied magnetic field.

Thus, in principle, recording MLD spectra is analogous to recording MCD spectra, but using linearly rather than circularly polarized light and with a different orientation of the applied magnetic field. Unfortunately, we find the MLD effect to be, typically, 1−2 orders of magnitude smaller than the corresponding MCD effect. Ideally, this should not be a problem as the experiment is configured and the detection system tuned so that the two kinds of signals are measured quite independently of each other. However, in reality, (i) instrument components are not ideal[18] and (ii) the relative alignment of the magnetic field and polarizing optics is inexact. As a result, distortion of the measured MLD signals due to an underlying MCD component is, in practice, sometimes clearly detected. Removal of both the MCD and natural LD components from the raw spectra was achieved by adopting the data collection protocol illustrated in Figure 2, where "a single spectral scan" actually involves the collection of three sets of data. It should be noted that the protocol takes advantage of the fact that changing the applied magnetic field orientation by 180° leads to MCD components of *opposite* sign, but MLD signal components of the *same* sign. Hence, any MCD contribution to the detected signals cancels in the final summation to obtain ΔA_{MLD}.

MLD−MCD Theory. The MLD differential absorption depends on three factors: (i) the difference of the squared matrix elements of the electric dipole operator components representing the transition probabilities for light polarized parallel and perpendicular to the magnetic field, *H*, (ii) the Boltzmann factor, and (iii) the line-shape factor, *f*. Expansion of this product with respect to field and temperature yields, ignoring higher order terms, the following general expression for the orientationally (powder) averaged nonsaturating MLD of molecules in solution:[12,13]

$$\frac{\Delta A_{\mathrm{MLD}}}{\epsilon} \approx \gamma \left\langle A_2\left(\frac{1}{2}\frac{\partial^2 f}{\partial \epsilon^2}\right) + \left[B_1 + \frac{C_1}{kT}\right]\left(-\frac{\partial f}{\partial \epsilon}\right) + \left[E_0 + \frac{F_0}{kT} + \frac{G_0}{(kT)^2}\right] f \right\rangle_{\mathrm{pa}} (\mu_{\mathrm{B}} H)^2 \quad (1)$$

where ϵ is the photon energy, γ is a product of fundamental constants, the terms $A-G$ are coefficients, k is the Boltzmann constant, T is the absolute temperature, μ_{B} is the Bohr magneton, and H is the applied magnetic field. To summarize the information content of the terms in eq 1, we first designate Zeeman interactions between sublevels which are degenerate in zero applied field as "inner state" and all other Zeeman interactions as "outer state" (these were previously termed "diagonal"

(3) Stephens, P. J.; Sutherland, J. C.; Cheng, J. C.; Eaton, W. A. In *The Excited States of Biological Molecules;* Birks, J. B., Ed.; Wiley: New York, 1976; Chapter D8, pp 434−442.
(4) Vickery, L. E. *Methods Enzymol.* **1978**, *54*, 284−302.
(5) Johnson, M. K.; Robinson, A. E.; Thomson, A. J. In *Iron−Sulfur Proteins;* Spiro, T. G., Ed.; Wiley: New York, 1982; Chapter 10, pp 367−406.
(6) Dooley, D. M.; Dawson, J. H. *Coord. Chem. Rev.* **1984**, *60*, 1−66.
(7) Dawson, J. H.; Dooley, D. M. In *Iron Porphyrins, Part III;* Lever, A. B. P., Gray, H. B., Eds.; Physical Bioinorganic Chemistry Series; VCH: New York, 1989; Chapter 1, pp 3−135.
(8) Cheesman, M. R.; Greenwood, C.; Thomson, A. J. *Adv. Inorg. Chem.* **1991**, *36*, 201−255.
(9) Thomson, A. J.; Cheesman, M. R.; George, S. J. *Methods Enzymol.* **1993**, *226*, 199−232.
(10) Solomon, E. I.; Pavel, E. G.; Loeb, K. E.; Campochiaro, C. *Coord. Chem. Rev.* **1995**, *144*, 369−460.
(11) Sutherland, J. C. *Methods Enzymol.* **1995**, *246*, 110−131.
(12) Kreglewski, M.; Vala, M. *J. Chem. Phys.* **1981**, *74*, 5411−5419.
(13) Bominaar, E. L.; Achim, C.; Peterson, J. *J. Chem. Phys.* **1998**, *109*, 942−950.
(14) Gerstman, B.; Austin, R. H.; Hopfield, J. J. *Phys. Rev. Lett.* **1981**, *47*, 1636−1639.
(15) Margoliash, E.; Frohwirt, N. *Biochem. J.* **1959**, *71*, 570−572.
(16) Antonini, E. *Physiol. Rev.* **1965**, *45*, 123−170.
(17) Nordén, B.; Davidsson, Å. *Acta Chem. Scand.* **1972**, *26*, 842−844.
(18) Davidsson, Å.; Nordén, B. *Chem. Scr.* **1976**, *9*, 49−53.

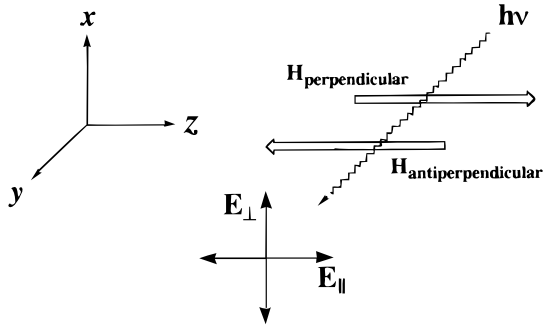

$$\Delta A_{perp} = \Delta A^{obs}_{perp} - \Delta A^{obs}_{zero}$$

$$\Delta A_{anti} = \Delta A^{obs}_{anti} - \Delta A^{obs}_{zero}$$

$$\Delta A_{MLD} = \left(\Delta A_{perp} + \Delta A_{anti}\right) \div 2$$

Figure 2. Experimental protocol for the measurement of cryogenic MLD spectra. The specified orientation of the electric vector (*E*) of the plane (linearly) polarized light is with respect to the applied magnetic field (*H*). The accumulation and processing of a "single spectral scan" (ΔA_{MLD}) actually involves the collection of three sets of data: (1) the measured signal (ΔA^{obs}_{perp}) with the field applied in the *perpendicular* direction with respect to the propagation direction of the incident light; (2) the measured signal (ΔA^{obs}_{anti}) with the field applied in the *anti-perpendicular* direction; (3) the measured signal (ΔA^{obs}_{zero}) with zero applied magnetic field. Subtraction of ΔA^{obs}_{zero} removes natural linear dichroism due to residual strain depolarization in the sample and spectrometer windows. The final summation removes any MCD components from the signal.

and "off-diagonal", respectively[13]). Remembering that both electronic ground and excited states must be considered, three of the coefficients (A_2, C_1, G_0) stem from only inner-state interactions, one (E_0) stems from only outer-state interactions, and the other two (B_1, F_0) stem from both.

The similarly derived expression for powder-averaged MCD under nonsaturating conditions is[19,20]

$$\frac{\Delta A_{MCD}}{\epsilon} \approx \gamma\left\langle A_1\left(-\frac{\partial f}{\partial \epsilon}\right) + \left[B_0 + \frac{C_0}{kT}\right] f\right\rangle_{pa} \mu_B H \qquad (2)$$

In this case, the A_1 and C_0 coefficients result from inner-state Zeeman interactions and only the B_0 coefficient is dependent on outer-state contributions. For paramagnetic samples, where temperature-dependent terms dominate upon cooling, it follows that cryogenic MLD is more useful for studying outer-state Zeeman interactions than cryogenic MCD.[13]

Results

Ferrocytochrome *c*. The near-ultraviolet-to-visible region of the electronic spectrum of biological hemes contains two distinct bands, the intense Soret (alternately called B, or γ) in the near-UV and the weaker Q (or α) in the visible. In addition, *b*-type and *c*-type hemes often contain a third well-defined β band of intermediate energy, which has been ascribed to a vibrational overtone (denoted Q_{0-1}) of the fundamental Q_{0-0} band.[21,22] The two lower energy features are evident in the 4.2 K visible region absorption spectrum of ferrocytochrome *c* (Figure 3A).[23] Unlike

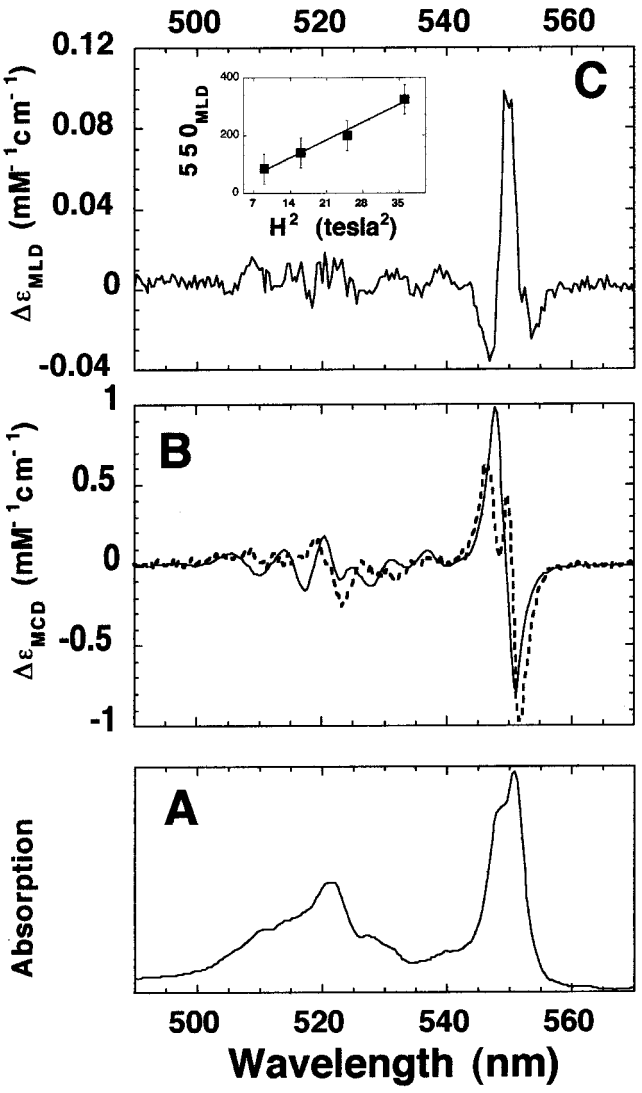

Figure 3. Cryogenic magnetooptical spectra of ferrocytochrome *c*, pH 7.4 in 20 mM 2-(*N*-morpholino)ethanesulfonic acid/HCl buffer, 50% (v/v) glycerol, 1.5 mM heme concentration, 0.3 mm path length: (A) electronic absorption spectrum at 4.2 K; the units of the ordinate axis are arbitrary; (B) MCD spectrum at 4.2 K and 1.0 T (solid line) and first derivative of the absorption spectrum in (A) (broken line, arbitrary units); (C) MLD spectrum at 4.2 K and 4.0 T, average of four spectral scans (inset: dependence of the 550 nm ferrocytochrome *c* MLD peak (millidegrees) on the applied magnetic field). Data were collected at 4.2 K sample temperature and applied magnetic fields of 3.0 T (4), 4.0 T (4), 5.0 T (1), and 6.0 T (1), where the values in parentheses are the number of individual spectra averaged in each case. The solid line represents the results of a linear regression analysis of the data (R = 0.992) which extrapolates through the origin within $^1/_2$ the computed standard error.

the room-temperature spectrum, the Q band becomes partially resolved into two components observed at about 547.5 nm (18 265 cm^{-1}) and 551 nm (18 150 cm^{-1}) upon cooling to cryogenic temperature. This corresponds to an excited-state splitting $\Delta = \sim 10^2$ cm^{-1} (see the Discussion).

(19) Stephens, P. J. *J. Chem. Phys.* **1970**, *52*, 3489−3516.
(20) Stephens, P. J. *Adv. Chem. Phys.* **1976**, *35*, 197−264.
(21) Platt, J. R. *J. Chem. Phys.* **1949**, *17*, 484−495.
(22) Platt, J. R. In *Radiation Biology*; Hollander, A., Ed.; McGraw-Hill: New York, 1956; Vol. 3, p 17.

(23) In general, the Soret band is difficult to measure at low temperature without severe distortion as it is invariably superimposed upon a sloping baseline due to Rayleigh scattering from the microstructure of the frozen glass. The scattering rapidly increases in the near-ultraviolet, and consequently, even at concentrations more dilute than those employed in the present study, samples are opaque (or nearly so) in the Soret region. Therefore, for most practical purposes, the reliable recording of this absorption band at cryogenic temperatures in semiaqueous glasses intended primarily for magnetooptical measurements is precluded.

The earliest theories that provided an interpretation for the heme transitions and their relative intensities were independently proposed by Platt, Simpson, and Kuhn.[21,22,24,25] These approaches concentrated on the π electrons of the porphyrin core and treated the macrocycle as a circular free-electron wire. The model system has C_∞ symmetry as a result of discarding the details of the peripheral structure. This idealization has the advantage that the angular momentum about the ring, L_Z, is a good quantum number, allowing the orbital eigenfunctions to be usefully characterized by integer M_L. The resulting orbital scheme has a singlet ground state ($M_L = 0$) and doubly degenerate excited states ($M_L > 0$). The electronic ground state corresponds to a filling scheme in which 18 electrons are packed in the closed-shell configuration $(0)^2(\pm1)^4(\pm2)^4(\pm3)^4(\pm4)^4$ with zero net angular momentum.[26,27] The lowest excited states correspond to promotion of one of the four electrons from the highest filled levels to either of the lowest empty levels. In this way, two doubly degenerate pairs of transitions are found: the dipole-forbidden $\mp4 \rightarrow \pm5$ ($\Delta M_L = \pm9$) and the dipole-allowed $\pm4 \rightarrow \pm5$ ($\Delta M_L = \pm1$). Hund's rule predicts that the lower-energy state corresponds to the $\Delta M_L = \pm9$ pair,[24] which is in accord with the observation of a relatively weak Q band in the visible and a stronger B band in the near-UV. This model has often been referred to as the Simpson model. Quite obviously, reliable determination of M_L is the key to testing the validity of this and alternative theoretical models for electronic structures of metalloporphyrins. Among the alternative models, we mention the four-electron, four-orbital model formulated by Gouterman,[27] which explicitly includes the effects of electron−electron repulsions. The four molecular orbitals considered in this model are labeled a_1 and a_2 (occupied in the ground state) and e_X and e_Y (empty in the ground state). The M_L states correspond to the combinations $|\pm4\rangle = (a_2 \pm ia_1)/\sqrt{2}$ and $|\pm5\rangle = (e_X \pm ie_Y)/\sqrt{2}$.[27b] The Slater determinants based on the complex orbitals provide a better description of the system than those based on the molecular orbitals only when the orbitals a_2 and a_1 differ in energy by an amount that is small compared to the energy splittings between configurations with different values for $|M_L|$.[27c] The large angular momenta of the Q-band excited states give rise to a substantial Zeeman splitting, which leads to intense (pseudo) A_1 term signals in the MCD spectra of low-spin ferrous hemes such as ferrocytochrome *c* (Figure 3B). More importantly for present purposes, there is a readily measurable MLD signature (Figure 3C) albeit 40 times weaker (comparing peak heights at the same applied field) than the corresponding MCD. The MLD signal intensity depends linearly on H^2 (inset in Figure 3C) in keeping with eq 1 and is temperature independent (not shown) as expected for a singlet ground state. The second-derivative (pseudo) A_2 term appearance of the spectrum is noteworthy. While it can readily be appreciated how the excited-state triplet example given in Figure 1 leads to a second-derivative signal, it is not immediately clear how this might also result from transitions between a ground-state singlet and an excited-state doublet (see the Discussion).

Deoxymyoglobin. In Figure 4 the 4.2 K electronic absorption (Figure 4A), MCD (Figure 4B), and MLD (Figure 4C) spectra of deoxymyoglobin are compared in the range 450−800 nm. Again, the MLD signal is readily measurable, and its intensity

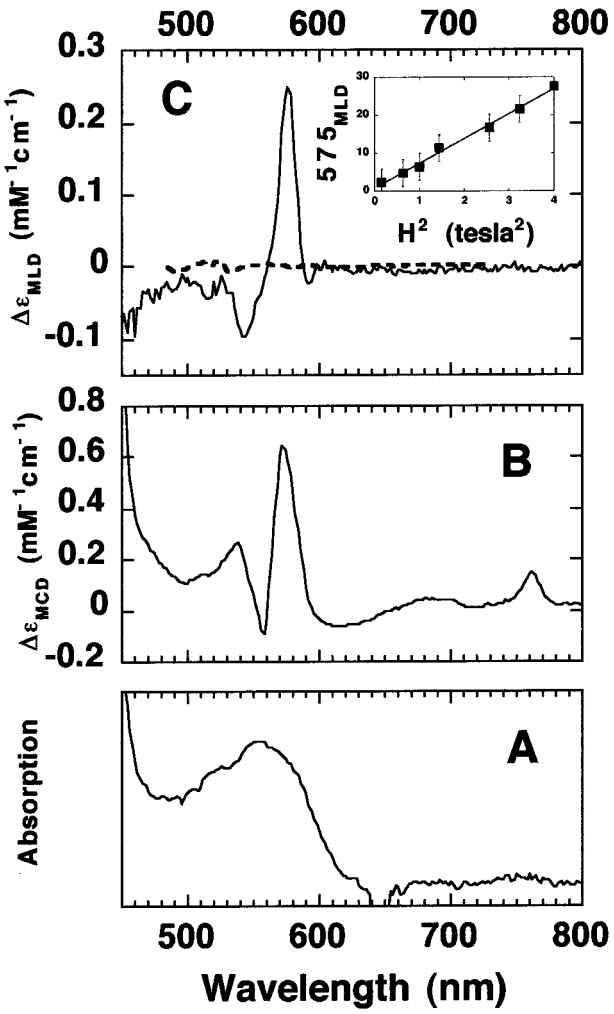

Figure 4. Cryogenic magnetooptical spectra of deoxymyoglobin, pH 7.4 in 20 mM 2-(*N*-morpholino)ethanesulfonic acid/HCl buffer, 50% (v/v) glycerol, 0.87 mM heme concentration, 0.5 mm path length: (A) electronic absorption spectrum at 4.2 K; the units of the ordinate axis are arbitrary; (B) MCD spectrum at 4.2 K and 5.0 T; (C) MLD spectra at 4.2 K and 7.0 T; deoxymyoglobin (solid line) and *ferri*cytochrome *c* (broken line) (inset: dependence of the 575 nm deoxymyoglobin MLD peak (millidegrees) on the applied magnetic field). Data were collected at 4.2 K sample temperature and applied magnetic fields of 2.0 T (4), 1.8 T (9), 1.6 T (9), 1.2 T (16), 1.0 T (16), 0.8 T (25), and 0.4 T (36), where the values in parentheses are the number of individual spectra averaged in each case. The solid line represents the results of a linear regression analysis of the data ($R = 0.997$) which extrapolates through the origin within $^1/_2$ the computed standard error.

varies linearly with H^2 (inset in Figure 4C) as predicted by eq 1. In this case, however, the MLD is only 4 times weaker than the corresponding MCD recorded under the same conditions of applied field and temperature. To date, this is by far the strongest MLD signal we have measured. Also, these bands are temperature dependent (not shown), indicating that the electronic ground state of the porphyrin moiety is strongly influenced by the paramagnetism of the coordinated high-spin ferrous ion, as previously indicated by MCD.[7,8] Consequently, in contrast to the situation in ferrocytochrome *c*, the observed spectral envelope cannot be accounted for by the temperature-independent A_2 term of eq 1.[28] Interestingly, the d−d bands[29,30]

(24) Simpson, W. T. *J. Chem. Phys.* **1949**, *17*, 1218−1221.
(25) Kuhn, H. *J. Chem. Phys.* **1949**, *17*, 1198−1212.
(26) Kobayashi, H. *J. Chem. Phys.* **1959**, *30*, 1361−1362.
(27) (a) Gouterman, M. In *The Porphyrins Physical Chemistry, Part A*; Dolphin, D., Ed.; Academic Press: New York, 1978; Vol. III, pp 1−165. (b) Gouterman, M. *J. Chem. Phys.* **1960**, *33*, 11523−11529. (c) Gouterman, M. *J. Chem. Phys.* **1959**, *30*, 1139−1161.

(28) It might not be appropriate to simply attribute the band shape of Figure 4C to the temperature-dependent terms in eq 1, since this expression was derived to describe transitions from either singlet ground states or degenerate manifolds under nonsaturating conditions.

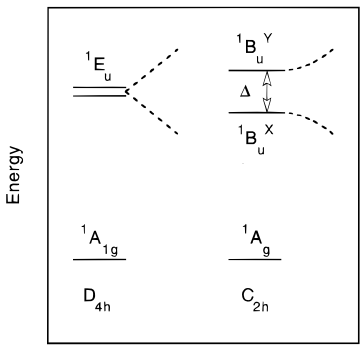

Figure 5. Initial and final states of the Q band under D_{4h} ($\Delta = 0$) and C_{2h} ($\Delta \neq 0$) symmetry. Broken curves indicate level energies in the presence of an increasing magnetic field.

between 600 and 800 nm evident in the MCD spectrum (Figure 4B) are apparently not present in the MLD (Figure 4C). The intensity ratio $\Delta\epsilon_{574}/\Delta\epsilon_{762}$ in the MCD spectrum is 4.3, whereas the analogous ratio ($\Delta\epsilon_{575}/\Delta\epsilon_{\sim 760}$) in the MLD spectrum must be greater than ~20 for the d−d transitions to have remained undetected. It was predicted[13] that the MLD signatures of transitions between orbital singlets in low-spin ferric hemes and other paramagnetic chromophores having an $S = {}^1/_2$ ground state are of lower intensity than those in systems with $S > {}^1/_2$. To test this prediction, attempts were made to record the MLD spectrum of ferricytochrome *c*, and these results clearly demonstrate (Figure 4C, broken line) that, if present, the MLD signals were at least an order of magnitude weaker than those of deoxymyoglobin.

Discussion

***S* = 0 Q-Band Theory.** In this section, eq 1 is evaluated in the framework of a three-state model for the Q band[27,31] in the case that both the initial and final states of the transition are spin singlets, $S = 0$. The ground state of the model is the orbital singlet $^1A_{1g}$ in D_{4h} symmetry, and the final state is the orbital doublet ^1E_u (Figure 5).[32] Ground and excited states are separated by an energy of about 1.8×10^4 cm^{-1} (550 nm). Under the influence of a crystal field of C_{2h} symmetry, ^1E_u is split into $^1B_u^X$ and $^1B_u^Y$ and the ground state is now labeled ^1A_g (Figure 5).[33] Our absorption measurements suggest the splitting energy Δ in ferrocytochrome *c* to be on the order of 10^2 cm^{-1} and justify the use of low-order perturbation theory to describe the effect of the Zeeman interaction between the two excited-state components.

As the ground state is nondegenerate, all temperature-dependent terms in eq 1 vanish: $C_1 = F_0 = G_0 = 0$. This leaves A_2, B_1, and E_0 as the only terms that can potentially contribute to the Q-band MLD. The Zeeman operator $-\vec{\mu}\cdot\vec{H} \equiv \mu_B(\vec{L} + 2\vec{S})\cdot\vec{H}$ simplifies to $\mu_B\vec{L}\cdot\vec{H}$ because the spin is zero in both the initial and final states of the transition. The Zeeman interaction in ^1E_u is axial ($g_X = g_Y = 0$) and is formulated in terms of an effective spin $S_{eff} = {}^1/_2$ Hamiltonian, $H_{Zee} = g_Z\mu_B H_Z S_Z$. Using the convention that lower and upper case labels refer to the laboratory and molecular frames, respectively, the magnetic field is applied along the laboratory *z* axis and H_Z is the field component along the molecular *Z* axis. The magnetic moment of the ^1E_u states is $\mu_B M_L = \mu_B(g_Z/2)$.

Under D_{4h} symmetry ($\Delta = 0$) there is a transition from an orbital singlet to an orbital doublet, $^1A_{1g} \rightarrow {}^1E_u$. By adopting the three-state model, we have implicitly assumed that the initial and final states are sufficiently isolated from other states (commonly denoted $|K_k\rangle$[12,13]) to ensure that terms originating from Zeeman interactions with those states (i.e., B_1 and E_0) are virtually zero. Consequently, the only remaining term is A_2. The powder average of this term is given by

$$\langle A_2\rangle_{pa} = -{}^1/_{30}(mg_Z)^2 \tag{3}$$

where $m \equiv \langle {}^1A_{1g}|m_X|{}^1E_u^X\rangle = \langle {}^1A_{1g}|m_Y|{}^1E_u^Y\rangle$.[35]

Under C_{2h} symmetry ($\Delta \neq 0$) there are two transitions, $^1A_g \rightarrow {}^1B_u^X$ and $^1A_g \rightarrow {}^1B_u^Y$, with energies differing by Δ. As the ground and excited states of the transitions are orbital singlets due to the prevailing crystal-field splitting, the orbital angular momentum is quenched in the three states of the model:

$$\langle {}^1A_g|\mu_z|{}^1A_g\rangle = \langle {}^1B_u^X|\mu_z|{}^1B_u^X\rangle = \langle {}^1B_u^Y|\mu_z|{}^1B_u^Y\rangle = 0 \tag{4}$$

In general, second-order Zeeman corrections in the line-shape function expansion are *not* negligible and must be combined with the field-independent transition probability and Boltzmann factor (the latter is here equal to 1) to produce a nonzero B_1 term (see eq 4c and footnote 41 of ref 13). Here, by accounting for the second-order Zeeman interactions between the components of the split ^1E_u, we find the B_1 terms given in eqs 5a and 5b (see Appendix A),

$$\langle B_1^{A\rightarrow X}\rangle_{pa} = +\frac{1}{60}\frac{(mg_Z)^2}{\Delta} \tag{5a}$$

$$\langle B_1^{A\rightarrow Y}\rangle_{pa} = -\frac{1}{60}\frac{(mg_Z)^2}{\Delta} \tag{5b}$$

where superscripts A, X, and Y indicate the ground state and excited-state lower and upper components, respectively. For Δ less than the spectral bandwidth, eqs 5a and 5b give rise to a pseudo-A_2 term

$$^1/_2\langle A_2^{pseudo}\rangle_{pa} f''(\epsilon) \approx -\langle B_1^{A\rightarrow X}\rangle_{pa} f'(\epsilon + \Delta/2) - \langle B_1^{A\rightarrow Y}\rangle_{pa} f'(\epsilon - \Delta/2) \tag{5c}$$

(derivatives with respect to ϵ are indicated by primes) which is independent of Δ and is given by the expression in eq 3

$$\langle A_2^{pseudo}\rangle_{pa} \approx \langle A_2\rangle_{pa} = -{}^1/_{30}(mg_Z)^2 \tag{5d}$$

The minus sign in eq 5d gives rise to a second-derivative spectrum in which the central feature is positive (Figure 6, top).

(29) Oganesyan, V. S.; Sharonov, Y. A. *Spectrochim. Acta* **1997**, *A53*, 433−449.

(30) Sharonov, Y. A.; Figlovsky, V. A.; Sharonova, N. A.; Mineyev, A. P. *Biophys. Struct. Mech.* **1983**, *10*, 47−59.

(31) Longuet-Higgins, H. C.; Rector, C. W.; Platt, J. R. *J. Chem. Phys.* **1950**, *18*, 1174−1181.

(32) Of course, strictly, the biological chromophores of interest have no symmetry. Here, in keeping with common practice, we assume the porphyrin π-orbital states can usefully be considered to be characterized by the D_{4h} or C_{2h} point groups.

(33) The irreducible representations $^1B_u^X$ and $^1B_u^Y$ are more often denoted $^1B_{1u}$ and $^1B_{2u}$ (e.g., see ref 27). The present notation was chosen to emphasize the $^1E_u^X$ and $^1E_u^Y$ parentage of the singlet states and more clearly associate these states with the coordinate axes of the molecular frame.

(34) Sutherland, J. C.; Axelrod, D.; Klein, M. P. *J. Chem. Phys.* **1971**, *54*, 2888−2898.

(35) Equation 3 can be derived either from eq A.1 of ref 13 by making an appropriate choice for the matrix elements and *g* factors or by direct powder integration of the A_2 term in eq 1.

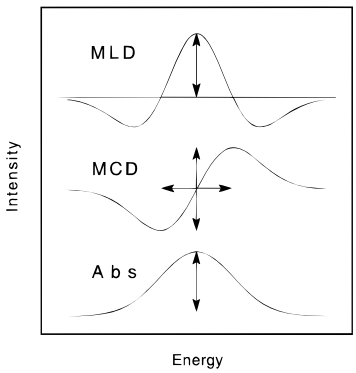

Figure 6. Gaussian band shape: bottom, absorption (f); center, MCD A_1 ($-\partial f/\partial\epsilon$); top, MLD A_2 ($-\partial^2 f/\partial\epsilon^2$). The vertical arrows indicate the amplitudes A_{Abs}, ΔA_{MCD}, and ΔA_{MLD} used in eqs 10−12. The horizontal arrow indicates the MCD peak-to-trough separation, W, used in eq 12.

Furthermore, it can be demonstrated that the powder average of the E_0 term is zero (see Appendix B)

$$\langle E_0^{\mathrm{A}\rightarrow\mathrm{X}}\rangle_{\mathrm{pa}} f(\epsilon+\Delta/2) + \langle E_0^{\mathrm{A}\rightarrow\mathrm{Y}}\rangle_{\mathrm{pa}} f(\epsilon-\Delta/2) \approx 0 \quad (6)$$

Thus, in the framework of the three-state model, the MLD of the Q band is predicted to yield a second-derivative spectrum for any value of Δ smaller than the bandwidth.

Under D_{4h} symmetry ($\Delta = 0$) the MCD of the $^1\mathrm{A}_{1g} \rightarrow {}^1\mathrm{E}_u$ transition has only a nonvanishing A_1 term (first-derivative term in eq 2) within the limits of the three-state model. Similarly, under C_{2h} symmetry ($\Delta \neq 0$) the MCD now consists of two oppositely signed B_0 terms pertaining to the transitions $^1\mathrm{A}_g \rightarrow {}^1\mathrm{B}_u^{\mathrm{X}}$ and $^1\mathrm{A}_g \rightarrow {}^1\mathrm{B}_u^{\mathrm{Y}}$ which together yield an MCD pseudo-A_1 term

$$-\langle A_1^{\mathrm{pseudo}}\rangle_{\mathrm{pa}} f'(\epsilon) \approx \langle B_0^{\mathrm{A}\rightarrow\mathrm{X}}\rangle_{\mathrm{pa}} f(\epsilon+\Delta/2) + \langle B_0^{\mathrm{A}\rightarrow\mathrm{Y}}\rangle_{\mathrm{pa}} f(\epsilon-\Delta/2) \quad (7a)$$

which is virtually independent of Δ and indistinguishable from the MCD A_1 term obtained under D_{4h} symmetry, provided Δ is smaller than the bandwidth.[34] The powder averaging yields the expression

$$\langle A_1^{\mathrm{pseudo}}\rangle_{\mathrm{pa}} \approx \langle A_1\rangle_{\mathrm{pa}} = {}^1/_3 m^2 g_Z \quad (7b)$$

Thus, provided the crystal-field splitting remains smaller than the bandwidth, both MLD and MCD spectra of the Q band retain their respective derivative features obtained under D_{4h} when the symmetry is lowered to C_{2h}.

The absorption band of the $^1\mathrm{A}_{1g} \rightarrow {}^1\mathrm{E}_u$ transition for a randomly oriented sample is given by

$$\langle A_{\mathrm{abs}}\rangle_{\mathrm{pa}} = {}^2/_3 \gamma m^2 f(\epsilon) \quad (8)$$

We approximate the normalized band shape $f(\epsilon)$ by a Gaussian function

$$f(\epsilon) = \Gamma^{-1}\pi^{-1/2} \exp[-((\epsilon-\epsilon_0)/\Gamma)^2] \quad (9)$$

where ϵ_0 is the transition energy in the absence of a magnetic field and the bandwidth at half-height is given by $2\Gamma(\ln 2)^{1/2}$. Using the definitions for the amplitudes given in Figure 6, we find for the (pseudo) A terms the absorption-normalized expressions

$$\frac{\Delta A_{\mathrm{MLD}}}{A_{\mathrm{Abs}}} = \frac{1}{20}\left(\frac{g_Z \mu_{\mathrm{B}} H}{\Gamma}\right)^2 \quad (10)$$

$$\frac{\Delta A_{\mathrm{MCD}}}{A_{\mathrm{Abs}}} = \left(\frac{2}{e}\right)^{1/2} \frac{g_Z \mu_{\mathrm{B}} H}{\Gamma} \quad (11)$$

In principle, the expressions in eqs 10 and 11 may be used to determine g_Z independently from the relevant pairs of spectroscopic results. However, at this juncture, a note of caution must be introduced. The parameters A_{Abs} and Γ in eqs 10 and 11 explicitly refer to the Gaussian envelopes where Δ is zero. When $\Delta \neq 0$, the apparent values of A_{Abs} and Γ deduced from the absorption spectrum are systematically too small and too large, respectively, as a result of band broadening due to splitting of the excited state (see Table 1). This phenomenon appears to have been reported,[36] but its nature misinterpreted in our opinion. Fortunately, dividing eq 10 by eq 11 and substituting $\Gamma = W/\sqrt{2}$ yields the additional absorption-independent relationship

$$\frac{\Delta A_{\mathrm{MLD}}}{\Delta A_{\mathrm{MCD}}} = \frac{e^{1/2}}{20} \frac{g_Z \mu_{\mathrm{B}} H}{W} \quad (12)$$

where W, the energy separation of the relevant MCD (pseudo) A_1 term peak and trough, is taken from the data of Figure 3B ($W = 112\ \mathrm{cm}^{-1}$). It is shown in Appendix C that eq 12 may be used in situations where Δ is either less than or comparable to the bandwidth.

Table 1. M_L Value, Gaussian Parameter (Γ), and Absorption Bandwidth Calculated as a Function of Selected Values for the Crystal-Field Splitting Δ at a Fixed Value of MCD Peak-to-Trough Energy Splitting W[a]

Δ (cm^{-1})[b]	M_L[c]	Γ (cm^{-1})[d]	width (cm^{-1})[e]
0	4.9	79.2	132
50	4.9	76.4	142
75	4.9	72.0	162
93[f]	4.9	66.2	188
100	5.0	62.5	197
110	5.4	51.2	195

[a] The value used for W is taken from experiment, 112 cm^{-1}. [b] $\Delta < W$; see Appendix C. [c] Obtained using eq C.5. [d] Obtained using eq C.3. [e] Width of absorption band at half the maximum height calculated with the values given for Δ and Γ given in the same row. [f] The absorption band has two maxima for Δ greater than this value.

Ferrocytochrome c. While the origin of the ferrocytochrome c second-derivative Q-band MLD has been formally demonstrated in the previous section, it remains to be understood from an intuitive point of view. To gain this further insight, it is useful to consider the interaction of individual molecules with the applied magnetic field (Figure 7). The first row of the figure shows three orientations of the applied field with respect to the molecular frame. The three situations represent a subset of the possible orientations that occur by applying a field to a randomly oriented ensemble of molecules. As before, Z is the magnetic anisotropy axis ($g_X = g_Y = 0$, $g_Z \neq 0$) of the molecule, and X and Y are the polarization directions ($\langle m_X\rangle = \langle m_Y\rangle \neq 0$, $\langle m_Z\rangle = 0$) of the Q band. The second row specifies the Cartesian contributions to $A_{\parallel} - \sum A_{\perp}$ for each direction of the field. Note that, in averaging the transition probability perpendicular to the applied field, there arises a geometrical factor of $^1/_2$ along each perpendicular Cartesian component ($\langle\cos^2\phi\rangle = {}^1/_2$), whereas

(36) Barth, G.; Linder, R. E.; Bunnenberg, E.; Djerassi, C.; Seamans, L.; Moscowitz, A. *J. Chem. Soc., Perkin Trans.* **1974**, *2*, 1706−1711.

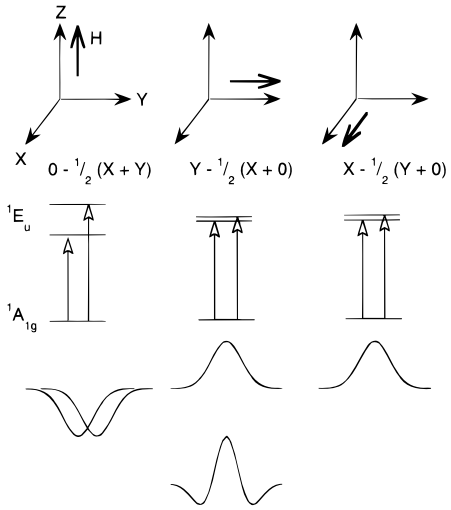

Figure 7. Schematic representation of powder-averaging the Q-band MLD, leading to a second-derivative spectrum (A_2 term). The following abbreviations have been used: $\langle m_X \rangle = X$ etc. Note that the intensity of the predicted MLD signal has been amplified with respect to the individual absorptions shown in the fourth row (see the text for further details).

along the parallel component the factor is unity. The third row indicates transitions and Zeeman splittings of the ^1E_u level for the field orientations considered in the first row. The fourth row gives the shapes, signs, and relative weights of the contributions to the Q-band MLD, with the resulting MLD spectrum obtained by summing the subspectra presented in the fifth row. We notice that the subspectra cancel exactly in zero applied field: the cancellation of linear dichroism by the incomplete powder-averaging procedure considered in the figure mimics the complete cancellation of linear dichroism in a randomly oriented sample.[13,37] In the presence of an applied field, however, the compounded spectrum appears as a second-derivative signal due to the Zeeman splitting when the field is applied along *Z*. It should be noted that the Q band of low-spin ferrous hemes is unusually sharp compared to the absorption bands of other metalloprotein derivatives. This property renders the measurement of the second-derivative MLD spectrum of Figure 3C possible, because the A_2 term is proportional to Γ^{-2}.

Using the relevant amplitude ratio obtained from the data of Figure 3B,C, we find by application of eq 12 that $M_L = g_Z/2 = 4.9 \pm 0.4$. The compounded error margin is estimated from the spread in the results of two independent sets of measurements and the uncertainty in *W*. The possible effect of large excited-state splitting ($\Delta = \sim 10^2$ cm^{-1}) on the determined value of M_L was explicitly investigated and found to be negligible (Table 1). In fact, only M_L values corresponding to $\Delta \leq 93$ cm^{-1} need to be considered as potential solutions, because for higher values of this parameter the absorption spectrum is split into separate bands for the individual transitions, leading to a spectrum with two maxima, in disagreement with the experiment.[38] Thus, within the limits of our present experimental uncertainty and the confines of the theoretical model, the 4.2 K MLD−MCD data show that $M_L \approx 4.9$ in ferrocytochrome *c*.

This result differs from the previous findings of others who estimated $M_L = 7.8$[39] and 7.9[40] for the same system from a combination of room-temperature MCD and absorption data. The former of these earlier studies assumed the band-shape equivalence of the first derivative of the absorption and MCD spectra. However, working at 4.2 K, it is quite clear that the first derivative of the absorption spectrum is different from the observed MCD (Figure 3B). The latter of the two earlier studies relied on a multiparameter fitting procedure to both data sets, and the analysis appears to have depended upon implicit assumptions concerning the insignificance of spectral overlap with the Q_{0-1} band (see Figure 4b of ref 40), possibly leading to overestimation of the Q_{0-0} transition bandwidth. It has been pointed out by Barth et al.[36] that the magnitude of M_L depends on the identity of the axial ligands present. Therefore, M_L may exhibit temperature-dependent variation due to changes in axial coordination. Clearly, this cannot explain the difference between the current and previous results because ligand substitution in cytochrome *c* is well-known to be accompanied by readily observable spectral changes,[7,8] which are not evident between 4.2 K and room temperature in the electronic spectra of ferrocytochrome *c*.

The combined MLD−MCD approach is a simpler (and thus preferable) method for determining M_L because (i) fitting is unnecessary, the required parameters being read directly from the spectra, (ii) the protocol is less dependent upon any implicit assumptions concerning the number and nature of additional interfering transitions, (iii) the ratio of experimental parameters taken is essentially independent of the excited-state splitting, and (iv) the method can be applied to numerous other kinds of scattering samples, like solid mulls, or biological membrane preparations. The present estimate of M_L is comparable to values determined for magnesium− and zinc−octaethylporphyrin derivatives,[36] but as the earlier study shows that the excited-state momenta are derivative dependent, a direct comparison is precluded. Interestingly, the most detailed available theoretical calculations[27] find the highest allowable angular momentum for the Q band to be about $5\hbar$, which is consistent with our current findings and differs from the $9\hbar$ predicted by the Simpson model.[24−26,31] In the context of the Gouterman model, our result for M_L implies that, if we compare the energy splitting between the orbitals a_2 and a_1 with the energy splittings between the configurations with different values for $|M_L|$ in ferrocytochrome *c*, the former quantity is relatively larger than it was previously believed to be on the basis of the value $|M_L| \approx 8$. In physical terms, this means that the magnetic-field-induced ring currents associated with the paramagnetic excited electronic states are less than was previously thought to be the case. It should be noted that the MLD−MCD method is not restricted to cryogenic temperatures, these conditions simply being chosen for convenience in our laboratory. Provided with the appropriate ambient-temperature bore magnet and enough sample, the procedure can be carried out at room temperature, where better optical transmission characteristics prevail and noise levels are consequently lower.

Deoxymyoglobin. To date, adequate theory has been developed to account for the MLD spectra of molecular chromophores with singlet and doublet ground states.[13] Ongoing efforts are aimed at developing theoretical formulations suitable for application to systems exhibiting higher ground-state multiplicities,[41] like deoxymyoglobin. Nevertheless, in the absence of a detailed analysis, straightforward comparison of the spectral data

(37) Nordén, B. *Appl. Spectrosc. Rev.* **1978**, *14*, 157−248.

(38) The Q-band absorption spectrum has a single maximum for $\Delta \leq \sqrt{2}\Gamma$ and a double maximum otherwise. The equality results if one takes the Γ value obtained from eq C.3 for $W = 112$ cm^{-1} and $\Delta \approx 93$ cm^{-1}. The shoulder observed near the maximum of the Q band in Figure 3A is due to differences in either bandwidths or amplitudes associated with the two transitions, which are close to the limit of resolution.

(39) Dratz, E. A. Ph.D. Thesis, University of California, Berkeley, 1966.

(40) Sutherland, J. C.; Klein, M. P. *J. Chem. Phys.* **1972**, *57*, 76−85.

(41) Bominaar, E. L.; Peterson, J. Manuscript in preparation.

of Figure 4C with those of Figure 3C leads to some important conclusions: (i) MLD can be observed for both diamagnetic and paramagnetic non-Kramers hemoprotein derivatives; (ii) the magnitude of the MLD signal obtained varies with the ground-state spin of the specific chromophore under study, indicating the effect to exhibit potentially advantageous selectivity; (iii) the MLD signals of at least some d−d transitions appear to be relatively weak compared to those of transitions involving ligand orbitals, which will likely prove diagnostically useful.

An especially noteworthy example of a system exhibiting a weak MLD spectrum is ferricytochrome *c*. Thus far, we have not measured any strong MLD signal associated with this or other systems having ground-state spin $S = {}^1/_2$. This is potentially a rather important observation. A significant limitation concerning the application of cryogenic MCD spectroscopy to metalloproteins is the extreme sensitivity of this technique to $S = {}^1/_2$ chromophores, like low-spin ferric hemes.[7,8] These sysems are generally electron-transfer centers in large protein complexes, and their intense spectral features tend to obscure any MCD signals arising from substrate-binding active sites. Many interesting metalloprotein derivatives are known in which the substrate-binding hemes have ground-state spins $S > {}^1/_2$. If MLD spectroscopy can routinely be used to extract magneto-optical signals from such centers in the presence of $S = {}^1/_2$ chromophores, then the concerted application of MCD and MLD to the study of metalloproteins will constitute an extremely powerful combination. The spectra of Figure 4C firmly support this suggestion.

Detection of a "magnetic-field-induced optical linear dichroism" at a single fixed wavelength has previously been reported for photolyzed carbonmonoxyhemoglobin maintained below 20 K,[14] but attributed to a magnetokinetic effect associated with recombination of the photolyzed ligand. In the present study, the data presented in Figure 4C can unambiguously be attributed to static MLD because the sample contained no photolytic ligand species. In fact, ligand photolysis and recombination of ferrous hemoprotein derivatives has been shown to be readily monitored by cryogenic MCD measurements.[42,43] Following a period of incubation at above 30 K, the lack of any time-dependent change of signal intensity in the 4.2 K spectrum of Figure 4B establishes that photolysis/recombination of some unidentified ligand did not occur in the current experiments.

Finally, preliminary MLD studies of samples other than hemoproteins have proved encouraging. Thus far, employing paramagnetic metalloprotein derivatives (40−60 μL sample volumes in the concentration range 0.1−2.4 mM) and model compounds, including both Kramers and non-Kramers ($S > {}^1/_2$) systems, data have been obtained from mononuclear iron centers and iron−sulfur clusters. Consequently, while the MLD experiment is significantly more troublesome to perform than MCD, the measurement does seem to have the necessary sensitivity as far as a range of metalloprotein systems is concerned, and therefore, it is to be anticipated that MLD spectroscopy will be of significance to many areas of biochemistry and biophysics.

Appendix A

The expressions for $\langle B_1 \rangle_{pa}$ in eqs 5a and 5b were derived from the expression for the MLD differential absorption[13]

$$\frac{\Delta A^{\xi}_{MLD}}{\epsilon} \propto [|\langle {}^1A_g|\vec{1}_z\cdot\vec{m}|{}^1B_u^{\xi}\rangle^0|^2 - |\langle {}^1A_g|\vec{1}_x\cdot\vec{m}|{}^1B_u^{\xi}\rangle^0|^2] f_H(\epsilon) \quad (\xi = X, Y) \quad \text{(A.1)}$$

where $\vec{1}_{x,z}$ are unit vectors along the laboratory axes *x*,*z*, by substitution of the ground- and excited-state functions for $H = 0$ (indicated by superscript 0), expansion in H of the field-dependent line shape function f_H (eq A.2), and taking the orientational average. The expansion of f_H in second order of the field yields

$$f_H = f + \langle {}^1B_u^{\xi}|\mu_z|{}^1B_u^{\xi}\rangle' \left(\frac{\partial f}{\partial \epsilon}\right) H^2 \quad \text{(A.2)}$$

The coefficient of the first-derivative term is given by

$$\langle {}^1B_u^{\xi}|\mu_z|{}^1B_u^{\xi}\rangle' = \frac{\langle {}^1B_u^{\xi}|\mu_z|K\rangle^0 \langle K|\mu_z|{}^1B_u^{\xi}\rangle^0}{W_K^0 - W_B^0} \quad \text{(A.3)}$$

and represents the second-order energy correction arising from the Zeeman interaction between ${}^1B_u^X$ and ${}^1B_u^Y$, the lower and upper levels of the split ${}^1E_u$ term, respectively. Then, for $({}^1B_u^{\xi}, K) = ({}^1B_u^X, {}^1B_u^Y)$, $W_K^0 - W_B^0 = \Delta > 0$, and $\langle {}^1B_u^X|\mu_z|{}^1B_u^X\rangle' > 0$, the ${}^1A_g \rightarrow {}^1B_u^X$ transition is shifted to a lower energy (see Figure 5). For $({}^1B_u^{\xi}, K) = ({}^1B_u^Y, {}^1B_u^X)$, $W_K^0 - W_B^0 = -\Delta < 0$, and $\langle {}^1B_u^Y|\mu_z|{}^1B_u^Y\rangle' < 0$, the ${}^1A_g \rightarrow {}^1B_u^Y$ transition is shifted to a higher energy. Equations 5a and 5b follow by straightforward integration over Euler angles, connecting the laboratory and molecular frames, of the expression obtained from eq A.1 by replacing f_H by eq A.3.

Appendix B

Diagonalization of $H_{Zee} + H_{CF}$, where H_{CF} is the crystal-field Hamiltonian which splits ${}^1E_u$, yields eigenstates ψ_1 and ψ_2. The states for $H \neq 0$ are related to the states ${}^1B_u^X$ and ${}^1B_u^Y$ for $H = 0$ by unitary transformation. The expression for E_0 obtained by using the exact eigenstates is

$$E_0^{A\rightarrow X} + E_0^{A\rightarrow Y} \approx \sum_{i=1,2} [|\langle {}^1A_g|\vec{1}_z\cdot\vec{m}|\psi_i\rangle|^2 - |\langle {}^1A_g|\vec{1}_x\cdot\vec{m}|\psi_i\rangle|^2] \left(f(\epsilon) + (-1)^i \frac{\Delta}{2}\frac{\partial f}{\partial \epsilon}\right) \quad \text{(B.1)}$$

First, let us consider the $f(\epsilon)$ term in eq B.1. The elementary relationship

$$\sum_{i=1,2} |\langle {}^1A_g|\vec{1}_\alpha\cdot\vec{m}|\psi_i\rangle|^2 = \sum_{i=1,2} \langle {}^1A_g|\vec{1}_\alpha\cdot\vec{m}|\psi_i\rangle\langle\psi_i|\vec{1}_\alpha\cdot\vec{m}|{}^1A_g\rangle \quad \text{(B.2)}$$

implies that the dependence of the coefficient of $f(\epsilon)$ on the eigenstates is given by the unity operator, $\sum_{i=1,2}|\psi_i\rangle\langle\psi_i|$, for the $\{{}^1B_u^X, {}^1B_u^Y\}$ space. As this operator is invariant under unitary transformations, it follows that the coefficient is independent of the field. As in the absence of a field ($H = 0$) the powder-averaged expression

$$\langle \sum_{i=1,2} |\langle {}^1A_g|\vec{1}_\alpha\cdot\vec{m}|\psi_i\rangle|^2 \rangle_{pa} \quad \text{(B.3)}$$

is independent of the orientation of the vector $\vec{1}_\alpha$, due to spatial isotropy of the randomly oriented samples studied here, the terms in the square brackets cancel in the powder average. Consequently, the $f(\epsilon)$ term in eq B.1 arising from Zeeman

(42) Greenwood, C.; Foote, N.; Peterson, J.; Thomson, A. J. *Biochem. J.* **1984**, *223*, 379−391.

(43) Greenwood, C.; Foote, N.; Peterson, J.; Thomson, A. *Biochem. Soc. Trans.* **1985**, *13*, 625−626.

interactions inside the split ^1E_u term is zero for any value of the field (see eq 6).

Second, the powder average of the derivative term in eq B.1 can be shown to be zero by explicit integration over the Euler angles, provided $\langle m_X \rangle = \langle m_Y \rangle$ (see text following eq 3). If the latter condition is not fulfilled, there arises a first-derivative (pseudo-B_1) term in addition to the A_2 term, which causes the MLD band to assume an asymmetric shape. As can be seen from Figure 3C, the left minimum of the MLD band is, indeed, slightly more depressed than the right minimum. However, the uncertainty in our present data precludes a quantitative analysis of this effect. We note that a B_1 term is zero at the maximum of the A_2 band and therefore does not affect the amplitude ratio given in eq 12.

Appendix C

In the Discussion, we have approximated the finite differential quotients

$$g(\epsilon) = [f(\epsilon - \Delta/2) - f(\epsilon + \Delta/2)]/\Delta \qquad \text{(C.1)}$$

$$h(\epsilon) = \Gamma[f'(\epsilon - \Delta/2) - f'(\epsilon + \Delta/2)]/\Delta \qquad \text{(C.2)}$$

which occur in the expressions for the MCD and MLD pseudo-A terms, by the corresponding infinitesimal differential quotients, i.e., the first and second derivatives of f (in eq C.2 the derivative with respect to ϵ is indicated by a prime), respectively. The Gaussian line-shape function (f) used in eqs C.1 and C.2 depends parametrically on Γ. As we are dealing in the case of ferrocytochrome *c* with a crystal-field splitting (Δ) that is on the same order of magnitude as the line width, it is necessary to establish the validity of this approximation. The peak and trough of the MCD first-derivative-type signal in eq C.1 are located at energies $\epsilon_0 \pm \epsilon_1$, and their separation is given by $W = 2\epsilon_1$. For any value of the crystal-field splitting $\Delta < W$, it is possible to determine a value for Γ for which the peak-to-trough separation of the theoretical spectrum in eq C.1 is equal to the directly observable quantity W for the Q-band MCD (note that for $\Delta \geq W$ there are no solutions). The solution can be expressed as

$$\Gamma = Wq^{1/2}\left[\ln\left(\frac{1+q}{1-q}\right)\right]^{-1/2} \qquad \text{(C.3)}$$

where we have used the definition $q = \Delta/W$. For a given value of W, the strong crystal-field limit, $\Delta \rightarrow W$, corresponds to the situation where the two absorption bands are completely separated. In the weak crystal-field limit, $\Delta \rightarrow 0$, eq C.3 simplifies to the expression $\Gamma = W/\sqrt{2}$ given in the text. Using eqs C.1−C.3, the amplitude ratio relevant to the MLD−MCD methodology (see Figure 6) can be expressed as a function of W and Δ

$$\left|\frac{h(0)}{2g(\epsilon_0 \pm \epsilon_1)}\right| = \frac{\Delta}{\Gamma}\exp\left[\left(\frac{W}{2\Gamma}\right)^2\right]\left(\exp\left[\frac{W\Delta}{2\Gamma^2}\right] - \exp\left[-\frac{W\Delta}{2\Gamma^2}\right]\right)^{-1} \qquad \text{(C.4)}$$

Equation C.4 simplifies to the factor $(e/2)^{1/2}$ in the limit $\Delta \rightarrow 0$. By replacing this factor with the rigorous expression given in eq C.4, we obtain in place of eq 12 the expression

$$\frac{\Delta A_{MLD}}{\Delta A_{MCD}} = \frac{1}{20}\left|\frac{h(0)}{2g(\epsilon_0 \pm \epsilon_1)}\right|\frac{g_Z \mu_B H}{\Gamma} \qquad \text{(C.5)}$$

where the quantity in magnitude signs is given by eq C.4 and Γ by eq C.3. Equation C.5 is a generalization of eq 12, valid for any allowed value of Δ. The values for $M_L = g_Z/2$ listed in Table 1 have been obtained from eq C.5 for different values of Δ, using experimental values for W (112 cm^{-1}) and the MLD and MCD amplitudes occurring in the ratio at the left-hand side of eq C.5.

In a somewhat similar manner, it can be shown that the value for M_L obtained from the MLD−MCD protocol is virtually independent of the instrument's bandwidth, provided the latter quantity does not exceed the limit above which the second-derivative signal appears as two separate first derivatives.

Acknowledgment. This work was supported by the National Science Foundation (Award Number 9506817 to J.P.) and Carnegie Mellon Faculty Development Fund (to J.P. and E.L.B.). Aviv Associates has been extraordinarily helpful in ensuring that the spectrometer performs with the sensitivity necessary for MLD and have absorbed some of the instrument development costs. David E. Holm undertook initial verification of the instrumentation's MLD capabilities at The University of Alabama. J.P. is indebted to Andrew J. Thomson who first interested him in the possibility of metalloprotein MLD and in whose laboratory at the University of East Anglia (U.K.) a feasibility study was carried out before assembling the presently employed equipment.

JA990174K